Feedback control of saccades on a model of a 3D biomimetic robot eye

Extended Abstract of the MSc. Dissertation

Rui Eduardo Marques Cardoso
Departamento de Engenharia Electrotécnica e de Computadores, Instituto Superior Técnico
Supervisors: Alexandre José Malheiro Bernardino

***Abstract*—The way the human brain controls movements is a widely studied subject. Considering the specific case of saccades, the trajectories the brain tends to choose from an infinite number of possible trajectories are highly stereotypical, in which non-linear dynamic properties are observed. Also, the fact that the eyes move in two degrees-of-freedom (DOF) from possible three, provided by six extraocular muscles, is a motivating aspect for studying these movements. The plane where the eyes move is called Listing's plane (LP). Seemingly, the brain considers a particular kind of disturbance which plays an important role in these properties of saccades, called signal-depentent noise (SDN). Here, a study on how saccades are controlled in the presence of SDN assuming the existence of internal feedback is presented. Simulations are carried out in a 3D biomimetic robot eye developed previously which was adapted to include a more realistic muslce model, SDN and a feedback control loop. Different methods are tested to obtain a valid linear parameterization of the eye model, which is then used to control stochastically the model using different optimization principles used in the literature through optimal feedback control. The non-linear dynamic properties were observed only under SDN conditions. The trajectories are fully contained in LP only if the final position is penalized for deviations to the LP. This fact is irrespective of the type of noise used.**

I. Introduction

Controlling human-like movements in such a sophisticated system as the brain does, where both actuators and sensors are biological mechanisms which carry in them such characteristic properties is a challenging problem and there is then room for plenty of research to be made. Here, the saccadic system is studied and, more precisely, an attempt to understand the reproduction of 3-dimensional eye movements is made by approaching the biological structure as a robotic system using engineering tools. The oculomotor systemis composed by six extraocular muscles which act in pairs, the eyeball and parts of the brain. It is responsible for all kinds of eye movements, in which there is the clear objective of keeping the point of interest centered in the *fovea*, the highest resolution part of the eyeball. The saccadic movements are focused here, as from the point of view of dynamics these are the most challenging. Saccades are quick and precise movements performed simultaneously by the eyes when an abrupt change in the point of fixation is required. Remarkably, these follow stereotypical trajectories which are confined to a plane where torsion is 0 [7] - the Listing's plane - and with a consistent relationship between amplitude, duration and velocity [1] - the main sequence. Several models have been developed to describe the system - starting in one-dimensional open loop models or with local feedback a number of more complicated models were estabilished with the goal of mimetizing correctly this class of eye movements.

To perform a saccade, the brain generates a control strategy in which the goal is to achieve a more rewarding state. Simultaneously, the change in state produced by a motor command is conditioned by a noise which grows with its size, called signal-dependent noise (SDN) [12], [5]. Nowadays, the saccadic system is thought to rely on a combination of planning and correctionof the movements. Several research works reported that, even though the brain preprograms our eyes'movement in order to reach the goal when stimulated by a visual signal, the generated trajectory mightchange midflight when the stimulus moves. Since saccades are such fast movements, the feedback information relies strongly on efferent copy of the motor commands. The way uncertainty affects sensory inputs as well as motor commands is acknowledged through learning which makes it possible to tune the motor responses to different sensory information.

We begin this work with a previously built mechanical prototype of a biologically inspired eye with six muscles. This system has, however, problems related with undesired effects emerging from the mechanical implementation (e.g vibrations) [11]. So, in order to proceed with the study of saccades, a model was developed in Matlab/Simulink from the mechanical prototype, which has allowed for the achievement of empirical proof of the saccadic system using optimal control in open-loop disregarding SDN, demonstrating that this framework emulates saccades with Listing's plane and main sequence behaviour [17].

II. Background

A. Oculomotor system

The oculomotor system, represented by the diagram in figure 1, consists of two main parts. On one hand it has a nonlinear plant - the eyes and their muscles - and on other hand an optimal controller - inside the brain.

Theoretically, there would be six degrees-of-freedom (DOF) in the plant. However, extraocular muscles act as agonist/antagonist pairs. Because of this only three DOF are used instead of the theoretically possible six.

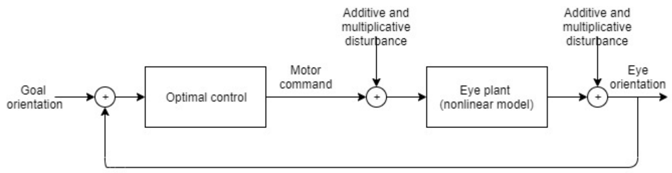

Fig. 1: The oculomotor system

To perform saccades, a strategy is developed by the brain in the superior colliculus [4], which uses its motor neurons to generate a signal by firing a burst of action potentials. It has been suggested in several models that the eye displacement is encoded in the brainstem and is used as an internal feedback signal.

Finally, there is another determinant factor in the oculomotor system when it comes to saccades, the presence of signal-dependent noise (SDN). This is a noise for which the standard deviation increases with the mean of the signal at stake.

B. Saccade Dynamics

1) Main sequence: The stereotypical relations between duration and amplitude as well as between peak velocity and amplitude for all healthy individuals form the main sequence. Several research works have shown that the duration of saccadic movements increase linearly with duration. On other hand, it has also been shown by various researchers that the peak velocity of saccades tends to increase linearly with amplitude, reaching a saturation value for large saccades. Later, studies have shown that there is also a typical relation between the movement amplitude and the asymmetry of saccadic velocity profiles, which is measured by their skewness[19].

These spatial-temporal relations which caracterize saccades are illustrated in figure 2.

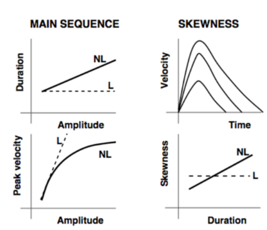

Fig. 2: Non-linear dynamics of saccades - the main sequence.

2) Eye orientation: As previously stated, the six extraocular muscles are mechanically arranged in such a way that the eye has 3 DOF rotating torsionally when about x, vertically for y and horizontally for z, from a primary position where all these angles are 0. The Donder's law states that the torsional component of the eye orientation is a function of the vertical and horizontal components, meaning that the eye has not three but only two DOF.

A further specification of Donder's law came with Listing's law, which states that with the head fixed and gazing at infinity in the primary position, any eye orientation can be reached by a single rotation about and axis in a plane orthogonal to the line of sight - the Listing's plane. Since we define the primary position as the position where the angles relative to three axes are zero, then Listing's law means that the torsion remains null in any other eye orientation and so, the Listing's plane is the set of orientations where there is no torsion. Nevertheless, if the primary position is not an eccentric position, although the orientation of the eye is still confined to a plane, this plane is no longer orthogonal to the line of sight, but tilted in the same direction of the line of sight half as much.

3) Curvature: Oblique human saccades exhibit almost perfectly straight trajectories, which suggests that the horizontal and vertical components may have a common command generator which is thus decomposed in these components. The model used in this study is three-dimensional and considers independent actuations in each of its dimension, intenting to replicate humans saccades by leaving these factors unconstrained. So, it is important to study the curvature of the saccades performed by the model in order to validate them. There are several methods to measure the curvature of saccades. Here, we will compute the correlation between velocity vectors in horizontal and vertical components of oblique movements. If the correlation is unitary, then the saccade is straight since its velocity components are perfectly scaled versions of each other. The goal is thus to have near-unitary correlation, but never unitary, in order to mimic saccades correctly.

C. Signal-dependent noise

Signal-dependent noise is commonly present in biological systems. This is a kind of disturbance in which the the standard deviation grows linearly as a function of the mean activation signal.

Regarding specifically the control of saccades, some research has also been made on the effect of SDN. The reason for the asymmetry in velocity profiles of saccades lies on the neural strategy of control, which tries to minimize variability [5] by producing large commands early in the movement in order to let variability dissipate naturally throughout the movement[14].

1) State-space representation: The state-space representation of a system consists of a mathematical model containing its state variables and relating its inputs and outputs by means of first-order differential equations. The equations below can describe a discretized version of a system perturbed by additive noise, ϵ_x and ϵ_y, and SDN, ϵ_u and ϵ_s:

$$\begin{aligned} \mathbf{x}^{(k+1)} &= A\mathbf{x}^{(k)} + B(\mathbf{u}^{(k)} + \epsilon_u^{(k)}) + \epsilon_x \\ \mathbf{y}^{(k)} &= H(\mathbf{x}^{(k)} + \epsilon_s^{(k)}) + \epsilon_y \end{aligned} \tag{1}$$

Here A represents the dynamic matrix, containing information about the system's dynamic properties, B represents the input matrix which translates the influence of the input, $\mathbf{u}$ into the dynamics and H is the output matrix, which transforms the state $\mathbf{x}$ into sensory readings $\mathbf{y}$. Note that m is the dimension of vector $\mathbf{u}$ - number of elements in the motor commands - and n is the dimension of vector $\mathbf{x}$ - number of elements defining the state.

The terms of additive noise, ϵ_x and ϵ_y, are defined as Gaussian random variables with zero-mean and variance Q_x and Q_y respectively:

$$\begin{aligned}\epsilon_x &\sim \mathcal{N}(0, Q_x)\\ \epsilon_y &\sim \mathcal{N}(0, Q_y)\end{aligned} \tag{2}$$

where Q_x and Q_y are $n \times n$ and $m \times m$ diagonal matrices with values q_x and q_y respectively in their diagonals.

The multiplicative noise terms are characterized with zero-mean magnitude and a variance that depends on the motor commands $\mathbf{u}$ and state $\mathbf{x}$ in the following form:

$$\begin{aligned}\epsilon_u^{(k)} &\sim \mathcal{N}(0, \sum_{i=1}^{m} C_i \mathbf{u}^{(k)} \mathbf{u}^{(k)T} C_i)\\ \epsilon_x^{(k)} &\sim \mathcal{N}(0, \sum_{i=1}^{n} D_i \mathbf{x}^{(k)} \mathbf{x}^{(k)T} D_i)\end{aligned} \tag{3}$$

One can state easily by analysing (1) that the noise introduces quantifiable variability into the system.

D. Feedback in saccades

The problem of generating motor commands to make some movement, like a saccade, is in some extent approached by our brain as an optimal feedback control problem:

- The movement has a cost as does our plan;
- A forward model gives a prediction of the outcome generated by some action;
- Some information about our state is retrieved during the execution.

The influence of feedback in saccades has been proven previously in different contexts [16] and in various models the internal feedback signal has been represented as an efference copy signal of position and/or velocity coming from the brainstem [4], [8], [13]. The fact that saccades rely mostly on an internal model while having such good performance makes us infer that this model must be accurate. As stated previously in II-C, SDN is critical in motor-planning [5] and has to be considered therefore by this model - through learning the brain is able to understand variability and its structure and how it affects the movement.

1) Optimal Feedback Control: Optimal control deals with finding the minima for a cost function of $\mathbf{u}$, the action variable, and $\mathbf{x}$, the state variable:

$$J(\mathbf{u}) = \Psi(x(T)) + \int_0^T L(\mathbf{x}, \mathbf{u}) dt \tag{4}$$

where

$$t \in [0, T]$$

$$\dot{\mathbf{x}} = f(\mathbf{x}, \mathbf{u})$$

However, the study of optimal control endowed with feedback relies more strongly in the field of stochastic optimal control for technical reasons - discrete spaces are proven to converge in a reasonable amount of time, unlike the continuous form. In order to understand the dynamics of these eye movements (better explained in **??**), some research has been made regarding the neuronal strategy behind them. While it is well-accepted that there is a trade-off between speed and accuracy originated by SDN, since it explains the main sequence [6], [4], [5], there is still some debate regarding other cost terms such as energy consumption, which has been claimed to be critical to the way the eye behaves in [9]. We have as base framework the approach in which the brain develops a control strategy regarding accuracy, energy consumption and speed:

$$J = J_x + J_u + J_p \tag{5}$$

The first term in (5), J_x, is responsible for penalizing the end-point inaccuracy:

$$J_x = \mathbf{x}^{(p)T} T \mathbf{x}^{(p)} \tag{6}$$

Here, T is a $n \times n$ diagonal matrix, and its values define the assigned penalization to each state-variable at the end of the movement. The second term, on other hand, represents the effort cost

$$J_u = \sum_{k=0}^{p} \mathbf{u}^{(k)T} L \mathbf{u}^{(k)} \tag{7}$$

Finally, the term J_p describes the temporal discount of reward:

$$J_p = \lambda \left(1 - \frac{1}{1 + \beta p}\right) \tag{8}$$

To obtain an optimum feedback policy, we consider a cost per time-step, $\alpha(k)$

$$\alpha(k) = \mathbf{u}^{(k)T} L \mathbf{u}^{(k)} + \mathbf{x}^{(k)T} T^{(k)} \mathbf{x}^{(k)} + \frac{\lambda\beta}{1 + \beta p} \tag{9}$$

It is thus useful to define a function which gives us the expected accumulated cost at each step - a function analogous to the *Bellman equation* with the difference that we want to minimize it:

$$v_{\pi*}(\mathbf{x}^{(k)}) = \underset{\mathbf{u}(k)}{min}\{\alpha^{(k)} + E[v_{\pi*}(\mathbf{x}^{(k+1)}) | \mathbf{x}^{(k)}, \mathbf{u}^{(k)}]\} \tag{10}$$

For any time-step, k, its value is given by the cost at that time-step $\alpha^{(k)}$ and the expected value of the state resulting from applying the optimal policy since the system is endowed with random disturbances. Todorov [18] proposed a form for eq. 10 at each time-step:

$$\begin{aligned}v_{\pi*}(\mathbf{x}^{(k)}, \hat{\mathbf{x}}^{(k)}) = \mathbf{x}^{(k)T} W_x^{(k)} \mathbf{x}^{(k)} +& \\ (\mathbf{x}^{(k)} - \hat{\mathbf{x}}^{(k)})^T W_e^{(k)} (\mathbf{x}^{(k)} - \hat{\mathbf{x}}^{(k)}) + w^{(k)}&\end{aligned} \tag{11}$$

Here, the influence of SDN affects the optimization of $v_{\pi*}$ since it alters the variance in the model.

$$\begin{aligned}G^{(k)} &\equiv (L + C_x^{(k+1)} + C_e^{(k+1)} + B^T W_x^{(k+1)} B)^{-1} B^T W_x^{(k+1)} A\\ \mathbf{u}^{(k)} &= -G^{(k)} \hat{\mathbf{x}}^{(k)}\end{aligned} \tag{12}$$

where,

$$\begin{aligned}C_x^{(k+1)} &\equiv \sum_i C_i^T B^T W_x^{(k+1)} B C_i\\ C_e^{(k+1)} &\equiv \sum_i C_i^T B^T W_e^{(k+1)} B C_i\\ D_e^{(k+1)} &\equiv \sum_i D_i^T H^T K^{(k)T} A^T W_e^{(k+1)} A K^{(k)} H D_i\end{aligned} \tag{13}$$

and

$$\begin{aligned}W_e^{(k)} \equiv&(A - AK^{(k)}H)^T W_e^{k+1}(A - AK^{(k)}H)\\&+ G^{(k)T}B^T W_x^{(k+1)}A\\W_x^{(k)} \equiv&T^{(k)} + A^T W_x^{(k+1)}A + D_e^{(k+1)}\\&- G^{(k)T}B^T W_x^{(k+1)}A\end{aligned} \tag{14}$$

We can easily see that control gains are inversely proportional to the motor noise and the energy penalization term - if the motor noise term is higher it is advantageous to produce smaller motor commands, and the same applies to the energy term.

E. Optimal Estimation

When controlling a system, the controller often does not have access to the full state-space. State observers combine the measured output of a system with the input which originated it to provide an estimate of the system's state.

That is the case of the Kalman filter (KF), which only provides state estimates using observations and the available information of an internal mathematical model of the device, but also filters disturbances.

$$\begin{aligned}K^{(k)} =&P^{(k|k-1)}H^T(HP^{(k|k-1)}H^T + Q_y\\&+ \sum_i HD_i\hat{\mathbf{x}}^{(k)}\hat{\mathbf{x}}^{(k)T}D_i^T H^T)^{-1}\end{aligned} \tag{15}$$

$K^{(k)}$ is the Kalman gain for time-step k, and $P^{k|k-1}$ is the prior state uncertainty. The state uncertainty is calculated in the following form, according to the model's dynamics:

$$\begin{aligned}P^{(k|k)} &= P^{(k|k-1)}(I - H^T K^{(k)T})\\P^{(k+1|k)} &= AP^{(k|k)}A^T + Q_x + \sum_i BC_i\mathbf{u}^{(k)}\mathbf{u}^{(k)T}C_i^T B^T\end{aligned} \tag{16}$$

The introduction of SDN in the system arises therefore a problem - the Kalman gains at each time step are dependent on the state and the motor command at the same time step. To solve this problem, Todorov [18] has sugested an iterative method for computing the Kalman gains.

III. Eye Model

A. Muscle model

The six extraocular muscles can be seen as three pairs of agonist/antagonist muscles acting in three distinct directions, x, y and z. In this work, we assume that, when it comes to force production, there are 3 identical agonistic systems which receive a neuronal signal (activation) and transform it into a force. The used model was taken from [15] and is as follows

$$\alpha_1\dot{f} + \alpha_2 f = u \tag{17}$$

However, this muscle model would be incomplete if it didn't consider the antagonist component of the pair. In other words, the antagonist muscle's elasticity and the influence it has on the system's dynamics. In fact, it is this part of the model which causes the coupling between the three dimensions in hand-eye orientation displacement causes the antagonist muscles to produce a force contrary to the sense of the displacement, which is modelled as an elastic for each muscle. Further explanation on the antagonist component of our muscle model is presented in the following section.

B. 3D Biomimetic robot eye model

The initial model in hands is a model of a mimetic robot of the eye where three motors are responsible for the movement of six points, P_i where strings are attached to replicate the six extraocular muscles. By moving these insertion points, tension is produced in these strings and therefore moving the eye. This model is adapted to introduce a muscle model with the agonistic properties described previously and antagonistic behaviour modeled by the strings.

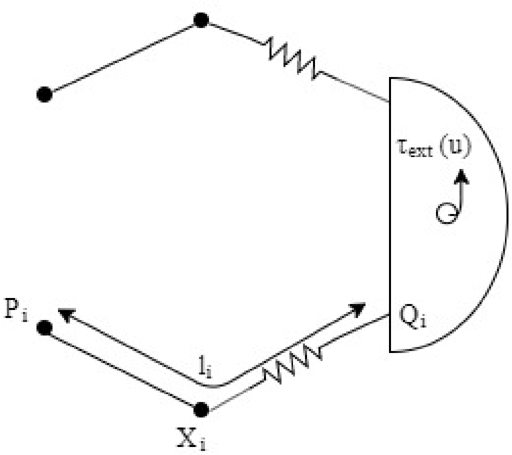

Fig. 3: Biomimetic robot eye one-dimensional model. P_i represents the points where elastics are fixed, X_i are points through which the elastics pass and Q_i are the insertion points of the elastics in the eyeball. These elastics represent the elastic part of muscles which act in pairs. The force these muscles produce is applied directly in the eyeball as an external force, τ_{ext}

When one of the muscles of each pair receives a neuronal signal demanding that a force is produced, it contracts, applying a force in the eyeball, while the other is extended and therefore creates a force in the direction contrary to the movement, as represented in figure 3 In the three-dimensional case, the forces created by the three muscle pairs form a torque which we called τ_{ext}

By introducing an input, a torque is created by the agonist muscles, moving the eyeball. The displacement of the eye originates a reaction on the antagonist muscles which create a torque in the opposite direction. The sum of the applied torques in the eyeball originates hence an angular acceleration according to Newton's 2nd law for rotations. By integrating it, the angular velocity is obtained which can be further integrated to obtain the new orientation of the eye. This procedure describes the developed simulator, whose diagram is in figure.

In order to design a feedback loop for our nonlinear model of the eye, it is necessary approximate its dynamic proper-

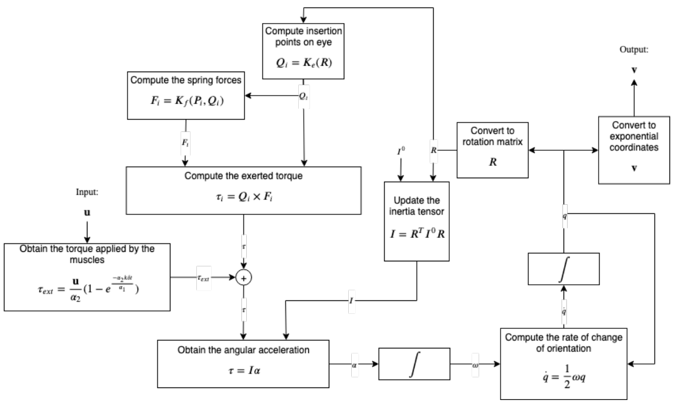

Fig. 4: Diagram of the nonlinear 3D model of the human eye

ties. For this, two main approaches were considered - using MATLAB/System Identification Toolbox and the analytical linearization of the described system. These are explained in detail below.

C. System Identification

Using Matlab's System Identification toolbox, the model of the robot was identified by loading in it a pseudo-random binary signal and observing its output's characteristics. The input signal has some restrictions which have to be obeyed to get a reasonable identification of the system. Here, the main parameters to take into account were both the input's period, which can't be too low to give the system time to stabilize before changing the input value again, and the input range in the 3 different channels.

In order to keep the relation between the hidden state, $\mathbf{x}$ and the output, $\mathbf{y}$, a a restriction about the values in the output matrix had to be imposed:

$$H = \begin{bmatrix} 1 & 0 & 0 & 0 & 0 & 0 \\ 0 & 0 & 1 & 0 & 0 & 0 \\ 0 & 0 & 0 & 0 & 1 & 0 \end{bmatrix}$$

This way, we can keep taking the values of x_1, x_3 and x_5 as the eye's angular position components in the eye reference frame axes x, y and z. However, there is no way to define the remaining state variables as velocities, which is a requirement if we want to apply sensor signal-dependent noise in the system. Since this problem arose, the solution found was to do something that suits us better not only regarding this problem but also in the time efficiency of parameterizing the system and the control of saccades in the nonlinear model itself - the analytical linearization of the non-linear system at a given point (x,y,z).

D. System Linearization

The state equations which rule the motion of the system are nonlinear. Through Jacobian linearization of the system, we can attain a linear approximation of the system for perturbations, δ, around some operating point using the following method:

$$\begin{gathered} \dot{\mathbf{x}} = \mathbf{f}(\mathbf{x}, \mathbf{u}) \\ \mathbf{f}(\mathbf{x}, \mathbf{u}) = \mathbf{f}(\mathbf{x}_0, \mathbf{u}_0) + \frac{df}{d\mathbf{x}}\bigg|_{\mathbf{x}_0, \mathbf{u}_0} \delta\mathbf{x} + \frac{df}{d\mathbf{u}}\bigg|_{\mathbf{x}_0, \mathbf{u}_0} \delta\mathbf{u} \\ \delta\mathbf{x} = \mathbf{x} - \mathbf{x_0} \\ \delta\mathbf{u} = \mathbf{u} - \mathbf{u_0} \end{gathered} \tag{18}$$

In the case of the operating point, $(\mathbf{x}_0, \mathbf{u}_0)$, being an equilibrium point, we know that the system is not moving and therefore we have

$$\mathbf{f}(\mathbf{x}_0, \mathbf{u}_0) = 0 \tag{19}$$

which leaves us with

$$\delta\dot{\mathbf{x}} = \frac{d(\mathbf{x} - \mathbf{x_0})}{dt} = \dot{\mathbf{x}} \tag{20}$$

Finally, substituting in (18) we arrive at a way of computing the linearized state equation of the system around the equilibrium point $(\mathbf{x}_0, \mathbf{u}_0)$

$$\dot{\mathbf{x}} = \mathbf{f}(\mathbf{x}, \mathbf{u}) = \frac{df}{d\mathbf{x}}\bigg|_{\mathbf{x}_0, \mathbf{u}_0} \delta\mathbf{x} + \frac{df}{d\mathbf{u}}\bigg|_{\mathbf{x}_0, \mathbf{u}_0} \delta\mathbf{u} \tag{21}$$

We have then:

$$\begin{gathered} A = \begin{bmatrix} \frac{df_1}{d\mathbf{v}} & \frac{df_1}{d\omega} \\ \frac{df_2}{d\mathbf{v}} & \frac{df_2}{d\omega} \end{bmatrix} \\ B = \begin{bmatrix} \frac{df_1}{d\mathbf{u}} \\ \frac{df_2}{d\mathbf{u}} \end{bmatrix} \end{gathered} \tag{22}$$

To compute these derivatives, some support from the MATLAB/Symbolic Math Toolbox was used given the extensiveness of these calculations.

In the end, we get a linearization of the continuous system which we want to control stochastically, so it has to be discretized. For this purpose, we use MATLAB/Control System Toolbox function *c2d()* with zero-order hold method and a sampling time of 0.001s.

E. Results

1) Muscle responses: The 1^{st} order agonist muscle system response was tested for different values of α_1, with fixed $\alpha_2 = 1$. We know from control systems theory that a first-order system has settling time of 3τ, and τ is the time constant, given in this case by $\tau = \frac{\alpha_1}{\alpha_2}$. So, the with fixed α_2, the settling time is dependent on the value of α_1 alone - as its value increases, the system becomes slower.

Analysing the response of the agonist and antagonist pair of muscles and the resulting force we simulated a neuronal step signal activating the lateral rectus - horizontal component in the positive sense of the force - and inspected the produced elastic torque.

As seen in figure 5, the step neuronal signal originates a step response of the agonist muscle, simulating its contraction, while the elastics produce a contrary torque stabilizing the total torque produced by the pair of muscles over a time period of roughly $130ms$.

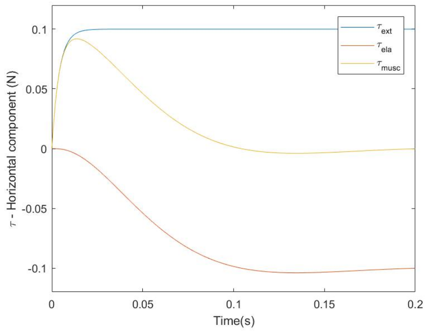

Fig. 5: Agonist/antagonist action of the muscle model. Here, τ_{ext} represents the lateral rectus as it simulates a contraction (agonist) in the positive sense of the horizontal component of the torque, while τ_{ela} simulates the action of the medial rectus (antagonist). The action of both results in a pulse, τ_{musc}

2) Identification and Linearization: The linearization around the equilibrium point $(\mathbf{x}_0, \mathbf{u}_0)$ was tested together with the model obtained from system identification. Figure 6 shows the comparison between the nonlinear system and the parameterization obtained from the two methods, performed Matlab's function *compare()*.

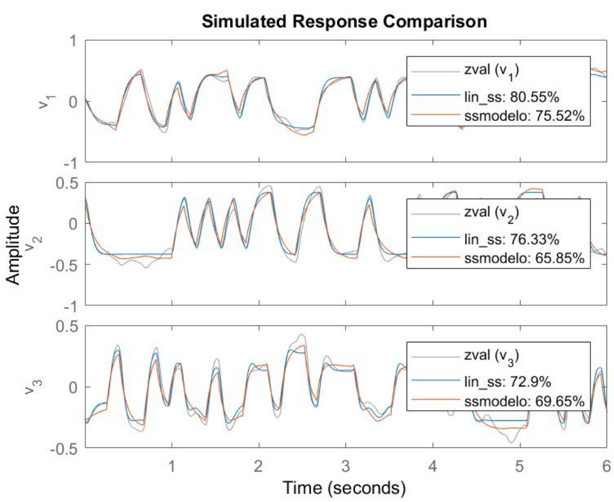

Fig. 6: Simulated response of IDS and LS superimposed in their 3 dimensions - the percentages represent the normalized mean squared goodness measure of each model in each dimension, the values of the output, v, are expressed in radians

The fitness value is calculated by

$$fit(i) = 1 - \frac{\|x_{zval}(:,i) - x(:,i)\|}{\|x_{zval}(:,i) - mean(x_{zval}(:,i))\|} \tag{23}$$

and it indicates how close are the systems' outputs relative to the measured output in the NLS, contained in $zval$. This result suggests that the NLS is better identified by the linearization than by Matlab's System Identification Toolbox.

IV. Optimal feedback control of saccades

A. Control design

To perform a saccade to a certain goal orientation $\mathbf{y_{ss}}$, firstly the expected value of the cost, $E[J(p)]$, is optimized by minimizing the value function given by (11), for a fixed movement duration, p. This process is repeated by searching in the whole plausible space of p. The movement duration which minimizes the cost is then selected, and the corresponding gains are used in the control.

We have, at this moment, defined the optimal controller and observer gains for each time-step, k, until the end of the saccade, p. This means, however, that when the saccade has reached its goal and the movement is over, $k = p$, we have no optimal gains to use in the observer and the motor command generator. Furthermore, it is necessary to introduce a reference to the system so that the error converges to zero, and not the state. So far, we have mentioned that the goal of a saccade is a specified orientation, but it is not just the orientation we are trying to control, but the whole state of the plant, $\mathbf{x}$, which consists not only of the orientation but also of the velocity.

Introducing a reference input in a feedback control loop is a well-studied problem in control theory. To implement this, we based ourselves on the explanation given in [3] on Reference Inputs with Estimators. Having in hands a type 0 system - a system in which the error will increase in steady-state - the urge to introduce a reference command input, $\mathbf{u}_{ff}$ arises together with the state reference. These contributions are added to the system employing two gains, N_x and N_u, which are obtained based on the system's dynamics

$$\begin{bmatrix} N_x \\ N_u \end{bmatrix} = \begin{bmatrix} A - I & B \\ H & 0 \end{bmatrix}^{-1} \begin{bmatrix} 0 \\ I \end{bmatrix} \tag{24}$$

By inputing the goal orientation in the system it is modified by these gains, generating a reference state, $\mathbf{s}$ and a reference motor command $\mathbf{u}_{ff}$.

Hence, this implies that at the end of the movement, as the feedback loop is not defined and thus will play no role in the control, the system is controlled only by the reference input. Since we are studying fundamentally the saccadic movement and not the subsequent period of fixation, the noise is removed at the end of the movement, p, for simplification purposes.

The final system has the following equations:

$$\begin{aligned}
&k \leq p \\
&\mathbf{x}^{(k+1)} = A\mathbf{x}^{(k)} + B(\mathbf{u}^{(k)} + \mathbf{u_{ff}} + \epsilon_u^{(k)}) + \epsilon_x \\
&\mathbf{y}^{(k)} = H(\mathbf{x}^{(k)} + \epsilon_s) + \epsilon_y \\
&\hat{\mathbf{x}}^{(k+1)} = A\hat{\mathbf{x}}^{(k)} + AK^{(k)}(\mathbf{y}^{(k)} - H\hat{\mathbf{x}}^{(k)}) + B(\mathbf{u^{(k)}} + \mathbf{u_{ff}}) \\
&\mathbf{u}^{(k+1)} = G^{(k+1)}(\mathbf{s} - \hat{\mathbf{x}}^{(k+1)}) \\
\\
&k > p \\
&\mathbf{x}^{(k+1)} = A\mathbf{x}^{(k)} + B\mathbf{u_{ff}} + \epsilon_x \\
&\mathbf{y}^{(k)} = H\mathbf{x}^{(k)} + \epsilon_y
\end{aligned} \tag{25}$$

Approach	Cost terms	Signal-dependent noise
1	AED	-
2	AED	✓
3	AD	-
4	AD	✓

TABLE I: Different approaches considered in the formulation of the optimal feedback control problem.

B. Optimal control approaches

As stated previously, the parameters which the brain tries to optimize when performing movements is a widely studied subject, but very few of these studies considered the specific case of optimal feedback control of saccades with SDN. However, there have been studies on this subject [14], [2] which are used here as the main background. In both these works, the cost assigned to saccades was considered to depend on three different aspects - Accuracy, Energy and Duration (**AED**).

$$J = J_x + J_u + J_p \tag{26}$$

In the framework of stochastic feedback control, this translates into the cost per step described by equation (9).

However, when we include SDN in the model, the term accountable for accuracy will have implicitly in it the influence of motor commands since its expected value depends on the variability of the state and the estimation error which is endowed with motor multiplicative noise.

This gives us the hint that the brain might not be minimizing effort but only endpoint accuracy and duration while considering the influence of SDN, as has been proposed previously [5], [10]:

$$J = J_x + J_p \tag{27}$$

which, in the stochastic framework leads us to the cost per step

$$\alpha(k) = \mathbf{x}^{(k)T} T^{(k)} \mathbf{x}^{(k)} + \frac{\lambda\beta}{1+\beta p} \tag{28}$$

We call this approach **AD** as it optimizes accuracy and duration, although with the presence of SDN we are implicitly optimizing effort as well.

Table I summarizes the approaches considered in this thesis to explain the control of saccades. In all these approaches it is necessary to tune variables T, λ and β which play a role in the cost functions. In the AED optimization approaches it is necessary to consider another variable correspondent to the effort penalization cost, L.

Moreover, to validate the correct behaviour of saccades in each approach, it is necessary to define a set of metrics with the human physiological ground which allow us to match the obtained results with the normal human saccade behaviour.

C. Saccade metrics

The factors to consider when evaluating the performance of our system in emulating the behaviour of the human eye in our system are the following:

- **Main sequence** - the stereotypical relation between amplitude and duration and between amplitude and peak velocity of saccades must be observed.
- **Skewness** - as the duration of saccades gets longer, their temporal velocity profiles tend to become more asymmetrical, with the peak velocity being attained early in the movement.
- **Listing's plane** - the eye torsion is zero in head-fixed saccades - $v_x = 0$.
- **Curvature** - Oblique saccades exhibit curvature in their trajectories.

D. Results

The values of variables T, λ and β were kept constant through the different approaches, varying only the energy penalty term, L and the motor noise matrix, C. It is important to note that the search for the optimal movement duration was made in multiples of two sampling periods, and the sampling period is $\Delta t = 0.001s$

1) Approach 1 - AED optimization without SDN: With the multiplicative noise matrices C and D to zero, and keeping the additive noise variances with the values $q_x = 0.001$ and $q_y = 0.001$, multiple saccades were simulated.

In figure 7, the relations between amplitude, duration and peak velocity are displayed. As expected, the compromise

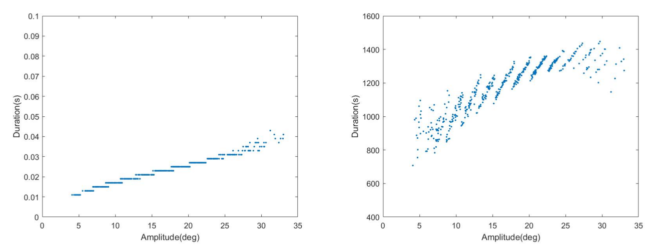

(a) Amplitude vs. duration (b) Amplitude vs. peak velocity

Fig. 7: Approach 1 - Main sequence

between accuracy, duration and effort originates movements with main sequence properties. Because the saccades have randomly generated initial and goal orientations, there is some variability in the velocity for movements with the same amplitude since the different directions lead to slightly different costs.

Horizontal saccades of different amplitudes were performed to check how their velocity profiles differ with amplitude. Figure 8 shows the effect of the effort penalization in this approach with the saturation on peak velocity, and the linear increase in duration with saccade amplitude. As expected, because this approach does not consider SDN, asymmetry in velocity profiles is not observed.

The saccade with the most curved trajectory from the set of oblique movements simulated has a correlation value between horizontal and vertical velocity components is $corr(\omega_y, \omega_z) = 0.996$, which is very high, meaning that this saccade is almost perfectly straight. The mean value of correlation in all the trials is 0.9982.

2) Approach 2 - AED optimization with SDN: In this approach signal-dependent noise was added to the simulator, with $c_i = 0.01$ for $i = 1, 2, 3$, i.e with equal noise magnitudes in the 3 input dimensions. All other conditions were the same.

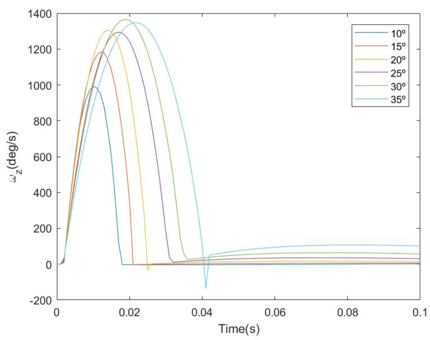

Fig. 8

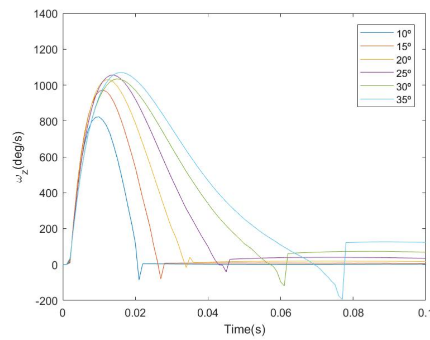

Fig. 10

The main sequence plots, seen in figure 9, have the desired shapes, demonstrating the linear relation between amplitude and duration (9a) and the saturating relation between amplitude and peak velocity (9b). However, these have differences when compared to the main sequence relations obtained in approach 1, where multiplicative noise was inexistent – the slope of the amplitude, duration is bigger and the peak velocity attains lower values for the same amplitudes. These differences reflect the influence of multiplicative noise in the system. By introducing this kind of disturbance , the system finds it more advantageous to produce lower motor commands, which results on a bigger movement duration and analogously in lower maximum velocities during each saccade.

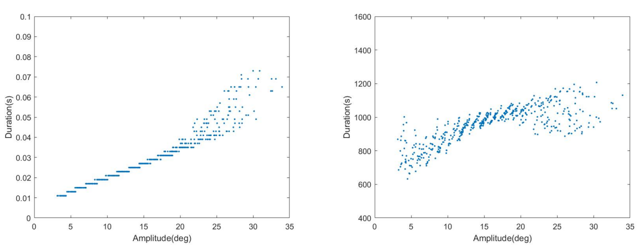

(a) Amplitude vs. duration (b) Amplitude vs. peak velocity

Fig. 9: Approach 2 - Main sequence

The temporal velocity profiles in figure 10 show the lower saturation values on the peak velocity as well as the increased difference between the durations of different amplitude saccades, confirming the conclusions attained by analyzing the main sequence plots. Also, it is noticeable that in high amplitudes the velocity profiles show asymmetry with the peak velocity being attained before half of the movement duration. This result confirms the expectation that the asymmetry in temporal velocity profiles is originated by SDN.

- **Curvature** The saccade obtained in the most curved trajectory trial has the correlation value $corr(\omega_y, \omega_z) = 0.975$. The mean value of correlation is roughly the same as in approach 1, but the trials in approach 2 have greater variability also in the correlation between velocity components given the introduction of SDN. In fact, the saccade presented here is more realistic relatively to the ones performed by humans.

E. Approach 3 - AD optimization without SDN

Approach 3 was experimented by removing the cost term on effort ($L = 0$), thus optimizing accuracy and duration. As in approach 1, SDN was set to zero and saccades with random initial and goal orientations were simulated.

The main sequence dependencies are in this approach, as expected, not followed. Analysing figure 11, although the duration seems to increase linearly with amplitude, the relation between amplitude and peak velocity is strange - bigger velocities are attained in lower amplitude saccades and in larger movements given the complete disregard on the values of the motor commands in this approach since there is no effort penalization nor signal-dependent noise implicitly in the accuracy term.

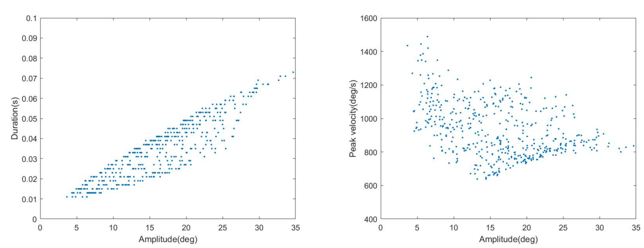

(a) Amplitude vs. duration (b) Amplitude vs. peak velocity

Fig. 11: Approach 3 - Main sequence

The temporal velocity profiles in figure 12 reflect this same effect, with the maximum velocity of the saccade being reached as soon as the movement begins as a result of the system finding itself in the state with the biggest value of error, to which the motor commands are proportional (see equation 25). Approach 3 fails to replicate both the non-linear dynamics and the temporal velocity profiles of human saccades.

The most curved saccade simulated here has the lowest correlation between velocity components in all the approaches, with the reasonably lower value of 0.8744. This is most likely caused by the fact that motor commands are not being minimized and the produced velocities are thus more irregular as seen in figure 12.

F. Approach 4 - AD optimization with SDN

Finally, we added SDN to the system and experimented it optimizing accuracy and duration cost terms in several random

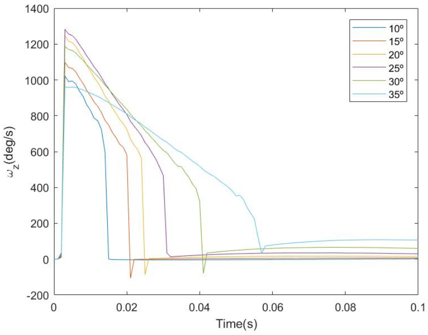

Fig. 12

saccades. The results are presented below.

As in approaches 1 and 2, the nonlinear dynamic properties of saccades are respected in this case as shown in figure 13. Although the effort is not constrained, the addition of motor signal-dependent noise is enough to make the main sequence relations similar to approach 2, where effort was minimized.

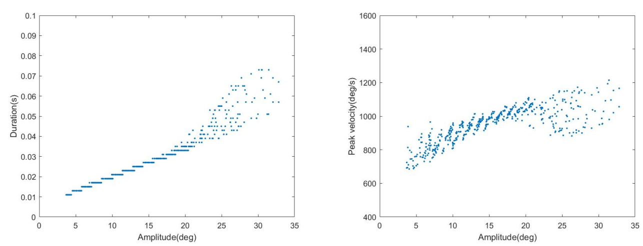

(a) Amplitude vs. duration (b) Amplitude vs. peak velocity

Fig. 13: Approach 4 - Main sequence

The obtained plots of velocity profiles for different amplitude horizontal saccades are shown in figure 14. These are very similar to the ones obtained using approach 2, presenting an increased asymmetry in bigger amplitude movements as well as peak velocity saturation, as expected since this approach also considers the influence of SDN.

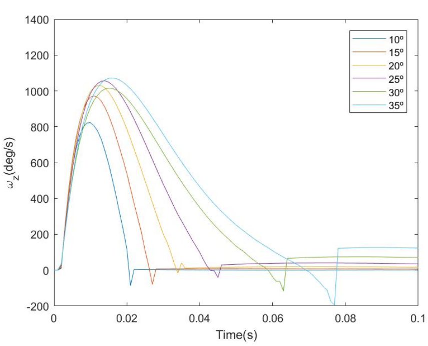

Fig. 14

• **Curvature** The curvature of the performed saccades is here very similar to what has been observed in Approach 2, confirming once more that these two approaches are highly connected. Both the minimum correlation trial and the mean of correlations have almost the same values: 0.973 and 0.986 respectivelly.

By matching the results obtained in this approach to the ones presented for approach 1 and 2, we can take the conclusion that, elegantly, the minimization of endpoint accuracy in a system endowed with noise that depends on the square of the motor commands, $\mathbf{u}^2$, produces the same realistic saccadic movements as optimizing effort, confirming the hypothesis suggested in [5], [10] which motivates this thesis. Moreover, all the approaches considered optimal feedback control and positive results were obtained in this framework, which is consistent with our assumption that the oculomotor system relies on a feedback loop.

G. Torsion constraint

We experimented recording torsion values from several saccades in two different conditions using approach 4 - regarding its final value and removing this weight in cost function.

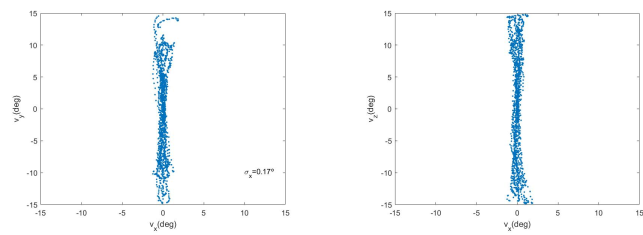

(a) Torsion vs. Vertical component (b) Torsion vs. Horizontal component

Fig. 15: XY and XZ planes obtained for several saccades constraining the endpoint value of torsion

The results obtained have shown that the eye stays in Listing's plane if its final orientation is constrained in this plane.

After removing the weight on torsion the results were, as expected, far from good - the torsion values are much higher in this case, and the eye does not move in a plane.

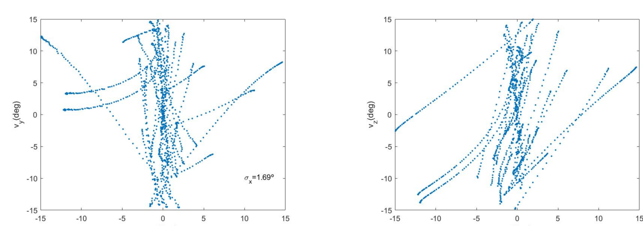

(a) Torsion vs. Vertical component (b) Torsion vs. Horizontal component

Fig. 16: XY and XZ planes obtained for several saccades disregarding the endpoint value of torsion

The results in figure 16b suggest tha this is apparently related with the coupling between the 3 dimensions in the model, especially the torsional and horizontal components, which results in highly coupled gains for u_x and u_z and thus the torsion values vary much in the favour of horizontal gains when it is not constrained. It is necessary, however, to do more research on this topic to confirm this hypothesis.

V. Conclusions

A. Discussion

Firstly, we used Matlab's System Identification Toolbox to obtain a linear parametrization of the model. However, this method was far from perfect, and another approach was taken by analytical linearization of the model, which proved to fit the needs of this work better considering the range of orientations near the equilibrium point where the system is linearized - It is both faster and more accurate than Matlab's toolbox.

After scrutinizing the performance of each approach in the different criteria, we concluded that the minimization of effort is redundant in the presence of SDN, as expected from an analytical perspective - in both cases, it is $\mathbf{u}^2$ which is being minimized. While in the absence of SDN it is necessary to minimize effort to obtain realistic saccades, in its presence, minimizing accuracy and duration is sufficient.

The results obtained on the Listing's plane analysis were inconclusive. By assigning a weight to the final torsional values, in an almost perfect Listing's plane emerged. By removing the weight on this component, however, the system stopped using exclusively 2 DOF, moving on the torsional dimension as well. This seems to be a consequence of using feedback controlling saccades in this system, with coupling between the 3 pairs of muscles but more research on this topic has to be made to confirm this hypothesis.

B. Future Work

Concerning possible future work to be done, it is important to mention the development of a model which can be used in the vicinity of other points and not just the equilibrium $(\mathbf{x}_0, \mathbf{u}_0)$, which can be done using the scripts developed in this thesis for the system linearization as a starting point.

Furthermore, the post-saccadic period of the simulation is a topic to be explored, which can be done by including the fixation period in the optimization.

Also importantly, the way the brain controls torsion in a feedback framework should be analysed into further detail. Moreover, the project in which this thesis is integrated, ORIENT I, aims to build a fully autonomous robot using audiovisual information to coordinate eye-head gaze orientation. So, after concluding the eye system, further work is planned on developing an auditory system and the integration of these two systems with a head-neck joint.

References

[1] A. T. Bahill, M. R. Clark, and L. Stark, "The main sequence, a tool for studying human eye movements," *Mathematical Biosciences*, vol. 24, no. 3-4, pp. 191–204, 1975.

[2] H. Chen-Harris, W. M. Joiner, V. Ethier, D. S. Zee, and R. Shadmehr, "Adaptive control of saccades via internal feedback." *The Journal of neuroscience : the official journal of the Society for Neuroscience*, vol. 28, no. 11, pp. 2804–13, 3 2008. [Online]. Available: http://www.ncbi.nlm.nih.gov/pubmed/18337410http://www.pubmedcentral.nih.gov/articlerender.fcgi?artid=PMC2733833

[3] G. F. Franklin, J. D. Powell, and M. Workman, "DIGITAL CONTROL OF DYNAMIC' SYSTEMS, G. F. Franklin and J. D. Powell, Addison-Wesley, London, 1980. Price: £10.75," *Optimal Control Applications and Methods*, vol. 6, no. 1, pp. 73–74, 1 1985. [Online]. Available: http://doi.wiley.com/10.1002/oca.4660060111

[4] H. H. L. M. Goossens and A. J. Van Opstal, "Optimal Control of Saccades by Spatial-Temporal Activity Patterns in the Monkey Superior Colliculus," *s*, vol. 8, no. 5, p. 1002508, 2012. [Online]. Available: www.ploscompbiol.org

[5] C. M. Harris and D. M. Wolpert, "Signal-dependent noise determines motor planning," vol. 413, no. September, pp. 396–400, 2001.

[6] ——, "The main sequence of saccades optimizes speed-accuracy trade-off," *Biological Cybernetics*, vol. 95, no. 1, pp. 21–29, 7 2006.

[7] T. Haslwanter, D. Straumann, B. J. M. Hess, and V. Henn, "Static roll and pitch in the monkey: Shift and rotation of listing's plane," *Vision Research*, vol. 32, no. 7, pp. 1341–1348, 1992.

[8] R. Jürgens, W. Becker, and H. H. Kornhuber, "Natural and drug-induced variations of velocity and duration of human saccadic eye movements: Evidence for a control of the neural pulse generator by local feedback," *Biological Cybernetics*, vol. 39, no. 2, pp. 87–96, 1981.

[9] A. A. Kardamakis and A. K. Moschovakis, "Optimal control of gaze shifts," *Journal of Neuroscience*, vol. 29, no. 24, pp. 7723–7730, 2009.

[10] J. Rn Diedrichsen, R. Shadmehr, and R. B. Ivry, "The coordination of movement: optimal feedback control and beyond."

[11] M. Ruiz and C. Lucas, "Construction and Characterization of a Biomimetic Robotic Eye Model with Three Degrees of Rotational Freedom : A Testbed for Neural Control of Eye Movements," no. October, 2017.

[12] R. A. Schmidt and et al, "Motor-output variability: A theory for the accuracy of rapid motor acts," *Psychological Review*, vol. 86, no. 5, pp. 415–451, 1979.

[13] C. A. Scudder, "A New Local Feedback Model of the Saccadic Burst Generator," Tech. Rep. 5, 1988.

[14] R. Shadmehr and S. Mussa-Ivaldi, "Optimal Feedback Control," in *Biological Learning and Control*. The MIT Press, 1 2012, ch. Optimal Fe, pp. 335–366.

[15] ——, "Cost of Time in Motor Control," *Biological Learning and Control*, pp. 307–334, 2013.

[16] D. L. Sparks and L. E. Mays, "Spatial localization of saccade targets. I. Compensation for stimulation-induced perturbations in eye position," *Journal of Neurophysiology*, vol. 49, no. 1, pp. 45–63, 1983.

[17] C. A. Tavares, "Control of Saccades with Model of Artificial 3D Biomimetic Eye," no. October, 2019.

[18] E. Todorov, "Stochastic optimal control and estimation methods adapted to the noise characteristics of the sensorimotor system," *Neural Computation*, vol. 17, no. 5, pp. 1084–1108, 2005. [Online]. Available: www.cogsci.ucsd.edu/

[19] A. J. Van Opstal and J. A. Van Gisbergen, "Skewness of saccadic velocity profiles: A unifying parameter for normal and slow saccades," *Vision Research*, vol. 27, no. 5, pp. 731–745, 1987.